2014

# A Comparison of Transient Heat-Pump Cycle Simulations with Homogeneous and Heterogeneous Flow Models

Christopher R. Laughman
*Mitsubishi Electric Research Laboratories, United States of America*, laughman@merl.com

# A Comparison of Transient Heat Pump Cycle Simulations with Homogeneous and Heterogeneous Flow Models

Christopher R. Laughman

Mitsubishi Electric Research Laboratories
Cambridge, MA 02139
laughman@merl.com

## ABSTRACT

This paper compares the effects of two different refrigerant flow modeling assumptions on the transient performance of vapor-compression heat pump cycles. These simulations are developed in the Modelica modeling language, which uses an acausal, equation-oriented approach to describe physical systems. The effect of the flow assumptions and specific slip ratio correlations on both the equilibrium operating point and the transient behavior of the cycle are demonstrated through these simulations. It is shown that equivalent simulations with different slip ratio correlations each have different equilibrium mass inventories, and that some aspects of the transient system behavior exhibit differences between the representative simulations. The effect of the software implementation on the model performance is also discussed.

## 1 INTRODUCTION

Dynamic models of vapor-compression heat pump systems are applicable for a wide variety of purposes, including component design and optimization, system-level design, controls development, and fault detection and diagnostics (FDD), and there has correspondingly been a wealth of research into different modeling approaches over the last 30 years (Rasmussen (2012), Li *et al.* (2014b)). This variety of modeling approaches arises due to the fact that the requirements and assumptions for a model depend heavily on its particular application. Of the available types of dynamic cycle models, those which incorporate distributed parameter representations of heat exchanger behavior are particularly useful for describing spatially dependent phenomena, such as the effect of nonuniform air velocities over the surface of heat exchangers, or the branching and joining of refrigerant pipes as a result of particular circuiting configurations. Such detailed models are useful for characterizing the detailed performance of heat exchangers, as well as understanding and constructing FDD algorithms for the detection of changes in the behavior of the overall cycle, e.g., detecting refrigerant overcharge or leakage from a cycle.

The equation-oriented modeling language Modelica (Modelica Association, 2014) has been gaining in popularity for the modeling of complex thermofluid systems (Li *et al.*, 2014a) due to its ability to encode detailed descriptions of multiphysics problems in a software representation, its inherently object-oriented construction, and the fact that it is an open language. Moreover, its ability to encode behavioral models into specific objects provides the user with a powerful abstraction concept; models can be created that allow different physical effects, such as gravitational head or viscous dissipation, to be easily added or removed. Like other equation-oriented modeling software packages, it uses a behavioral modeling paradigm (Willems, 2007), and employs computer algebra techniques to simplify and solve systems of differential algebraic equations (DAEs), such as those that represent the behavior of of heat exchangers, to produce a set of ordinary differential equations that can be simulated with state-of-the-art solvers, such as DASSL and Radau IIa (Cellier and Kofman, 2006).

One of the many decisions that must be made when developing transient models of thermofluid systems is the method for describing the two-phase flow pattern. A common assumption used in these system models is that both phases flow at the same velocity, otherwise referred to as a homogeneous flow pattern, while the relaxation of this assumption results in different phasic velocities, or a heterogeneous flow pattern (Ghiaasiaan, 2007). While homogeneous flow models are generally reasonable for dispersed flow patterns (e.g., bubbly and spray flow), they are generally not valid for separated flow patterns (e.g., stratified and annular flow) since for these systems (Kolev, 2005, p.151),

$$1 \leq S \leq \sqrt{\frac{\rho_L}{\rho_G}}, \tag{1}$$

where $S = v_G/v_L$. The choice of flow model used to describe a vapor compression system is important because some

of the system's equilibrium characteristics, such as its total mass inventory, are strongly related to the flow regime. One particularly common type of heterogeneous flow model is known as a slip flow model, in which it is assumed that mass transfer across the phasic interface takes place without an accompanying momentum transfer. This model can be formulated as a set of equations describing the two-phase mixture with an extra set of closure relations to relate the different phasic properties to each other, and is consequently much simpler than a complete multifluid model.

Though much of the extant literature describing distributed parameter models of vapor compression systems in Modelica assumes a homogeneous flow model, e.g., Bonilla *et al.* (2012) and Mortada *et al.* (2012), there has been some prior work in using Modelica to develop slip flow models of heat exchangers for vapor compression systems. In his thesis, Bauer (1999) developed two different slip flow models of the dynamics of a evaporator. These models were validated on a shell-in-tube heat exchanger; this validation demonstrated both that homogeneous flow models were inadequate to describe the evaporator's mass inventory, and that the performance of his different slip flow models were comparable. More recently, Kærn (2011) coupled a slip flow evaporator model to a moving-boundary condenser model and static compressor and expansion valve models to explore and understand the effects of maldistribution in evaporator coils.

Other literature that describes transient models of vapor-compression systems, e.g., Li and Alleyne (2010) and Kapadia *et al.* (2009), does include the use of correlations describing the slip ratio $S$ in their description of the two-phase flow dynamics. These models typically choose a slip correlation based upon a combination of the the correlation's accuracy and its simplicity. However, though a number of slip correlations have been described in the literature, e.g., Ma *et al.* (2009) and Harms *et al.* (2003), each of these correlations is often only compared to the experimentally measured void fraction of either a single heat exchanger or the overall cycle. It thus remains to be seen if the transient behavior of a vapor compression system model is dependent upon the slip correlation used, or if all of the slip correlations yield the same overall system dynamics.

This paper has two principal objectives. First, a set of distributed parameter models of the vapor compression cycle with both homogeneous flow and slip flow models is developed in Modelica. This makes it possible to examine the effect of the flow model on the equilibrium operating point of the closed cycle and better understand and demonstrate the impact of these modeling assumptions on the system dynamics generally and the distribution of the refrigerant mass specifically. Second, the slip ratio models of Zivi (1964), Smith (1969), and Premoli *et al.* (1971) are each implemented in otherwise identical versions of the complete cycle model; the resulting comparison of the outputs of each of the four transient system models will provide increased understanding of the effect of a specific slip flow model on the overall system dynamics. Modelica is particularly well suited to this type of investigation because the different slip ratio models can be individually replaced in the overall cycle model without changing any of its other behavioral characteristics.

Section 2 of this paper contains descriptions of the component models needed to develop a complete cycle model of an air-to-air heat pump, including a description of the finite control volume models of the heat exchangers with a formulation of the slip flow terms. Salient details of the implementation in Modelica are then described in Section 3, while Section 4 illustrates a selection of results from the complete cycle simulations to illustrate the differences between the modeling approaches. Finally, conclusions and potential areas of further exploration are discussed in Section 5.

# 2 MODEL DESCRIPTION

A vapor compression cycle model requires component submodels for the heat exchangers, compressor, and expansion valve. Because of the complexity of the two-phase flow model, this section begins by describing the relations between the phasic and mixture fluid properties in a control volume, and this is followed with a discussion of the conservation equations for a control volume. These models are then combined to form a set of equations that characterize the behavior of the heat exchangers. Finally, the models of the compressor and expansion valve are described at the end of this section.

The underlying physical dynamics of the refrigerant flow through the heat exchangers is governed by a set of partial differential equations (PDEs) that interrelate the mass, momentum, and energy balances in the fluid. Because of the difficulty of solving these PDEs in general, the approach used in this paper discretizes the PDEs, resulting in a set of nonlinear ordinary differential equations (ODEs) that must be solved with a numerical integration routine. These balance equations do not completely define the set of equations, however; algebraic equations of state are needed to describe the relations between the thermodynamic and transport properties of the refrigerant, and experimentally derived closure

relations are also needed to define some of the important interactions, such as the relationship between the heat flux and the temperature difference. This full set of mathematical relations thus comprises a set of DAEs.

A number of assumptions were made in the construction of the heat exchanger model, including the fact that there are no gradients in either the refrigerant properties or the velocity field in the radial or $\theta$ directions, that each control volume is in thermodynamic equilibrium, that there is no thermal conduction along either the refrigerant or the heat exchanger wall in the $z$ direction, that the wall temperature in each control volume is uniform, that the potential energy change across the heat exchanger is negligible, and that the dry air medium can be modeled as an ideal gas.

For a given volume containing two-phase refrigerant in the pipe, an extensive property $\Psi$ can be written as the mass-weighted mixture of the constituent phasic properties by averaging over the phasic volumes, e.g.,

$$\Psi = \Psi_G + \Psi_L \tag{2}$$

$$\psi = \Psi / M_{total} = \psi_g M_g + \psi_L M_L = x\psi_G + (1-x)\psi_L, \tag{3}$$

where $x$ is referred to as the static quality, or

$$x = \frac{M_G}{M_G + M_L} = \frac{M_G}{M_{total}}. \tag{4}$$

The same intensive property $\psi$ can also be written as

$$\psi\rho V = \psi_G \rho_G V_G + \psi_L \rho_L V_L \tag{5}$$

$$\psi\rho = \gamma\psi_G\rho_G + (1-\gamma)\psi_L\rho_L, \tag{6}$$

where the void fraction $\gamma$ can be written as

$$\gamma = \frac{V_G}{V_G + V_L} \simeq \frac{A_G}{A_G + A_L}, \tag{7}$$

and the second equality applies when computing the void fraction over a control volume with a fixed length. This formulation of the property relations assumes that flow field containing both phases at $z_0$ is frozen at a point in time, and the spatial average that can be taken over this frozen flow field is also representative of the ensemble average at this point taken over a period of time (Ishii and Hibiki, 2011).

These expressions make it possible to write down aggregate intensive properties as a function of their phasic components, either in terms of the void fraction or the static quality, e.g.,

$$\rho = \gamma\rho_G + (1-\gamma)\rho_L \tag{8}$$

$$h = xh_G + (1-x)h_L \tag{9}$$

$$v = xv_G + (1-x)v_L. \tag{10}$$

A relation between the void fraction and the static quality can also be formulated by noting that

$$x = \frac{M_G}{M_{total}} = \frac{\rho_G V_G}{\rho V} = \gamma\frac{\rho_G}{\rho}. \tag{11}$$

Because it will be used in the energy balance, it is also helpful to define a quantity referred to as the flow quality $\dot{x}$ to describe the ratio of the phasic mass flow rates, e.g.,

$$\dot{x} = \frac{\dot{m}_G}{\dot{m}_G + \dot{m}_L} = \frac{\gamma\rho_G v_G}{\gamma\rho_G v_G + (1-\gamma)\rho_L v_L} \tag{12}$$

$$= \frac{xv_G}{xv_G + (1-x)v_L}. \tag{13}$$

Equation 12 demonstrates the fact that the static quality is equal to the flow quality only when the gas and liquid velocities are equal. It is also helpful to express the void fraction $\gamma$ in terms of the flow quality, e.g.,

$$\frac{1}{\gamma} = 1 + \left(\frac{1-\dot{x}}{\dot{x}}\right)\left(\frac{v_G}{v_L}\right)\left(\frac{\rho_G}{\rho_L}\right). \tag{14}$$

The states that are chosen for the system are the pressure and the *in situ*, or density-weighted, enthalpy, based upon the frozen flow field (Equation 9). This *in situ* enthalpy differs from the "mixed-cup", or flow-weighted, enthalpy, which is defined as

$$\dot{m}\bar{h} = \dot{m}_G h_G + \dot{m}_L h_L \tag{15}$$

$$\bar{h} = \dot{x} h_G + (1 - \dot{x}) h_L, \tag{16}$$

Both of these different enthalpies will appear separately in the conservation equations, and are only equal if $x = \dot{x}$.

By using these mixture property relations, the mass, momentum, and energy balance equations can be written down for the two-phase medium. These balance equations for each one-dimensional individual control volume can be formulated in a relatively straightforward manner under a homogeneous flow assumption, as discussed in White (2008) and in Franke *et al.* (2009b) in a more Modelica-specific context, are

$$\frac{\partial(\rho A)}{\partial t} + \frac{\partial(\rho A v)}{\partial x} = 0 \tag{17}$$

$$\frac{\partial(\rho v A)}{\partial t} + \frac{\partial(\rho v^2 A)}{\partial x} = -A\frac{\partial p}{\partial x} - F_f \tag{18}$$

$$\frac{\partial(\rho(u + v^2/2)A)}{\partial t} + \frac{\partial(\rho v(h + v^2/2)A)}{\partial x} = \frac{\partial Q}{\partial x}, \tag{19}$$

The friction force $F_f$, is equal to the product of the cross-sectional area at location $z_0$ multiplied by the equivalent frictional pressure drop (Equation 20),

$$\Delta p_{fric} = \zeta \frac{L}{D}\frac{\rho v^2}{2}. \tag{20}$$

The dimensionless friction factor $\zeta$ is calculated for flows with Re < 2000 by using the Hagen-Poiseuille law (Stephan, 2010), e.g.,

$$\zeta_{lam} = \frac{64}{\mathrm{Re}}, \tag{21}$$

while the Blasius correlation (Stephan, 2010) for smooth-walled pipes is used for flows with Re > 6000, e.g.,

$$\zeta_{turb} = \frac{0.3164}{\sqrt[4]{\mathrm{Re}}}, \tag{22}$$

and a cubic polynomial was used to interpolate between these two regions in $\log_{10}(\mathrm{Re})$ vs. $\log_{10}(\zeta)$ coordinates (Elmqvist *et al.*, 2003) to generate a smooth continuous function $\zeta$ for all values of Re. Similar techniques can be used to describe the two-phase multipliers needed to describe pressure drops in two-phase flow; such methods will be used to improve future versions of these models.

An alternative energy balance (Elmqvist *et al.*, 2003) can be formulated by multiplying the momentum balance by the fluid velocity $v$ and subtracting it from the original energy balance, resulting in

$$\frac{\partial(\rho u A)}{\partial t} + \frac{\partial(\rho v h A)}{\partial x} = vA\frac{\partial p}{\partial x} + vF_f + \frac{\partial Q}{\partial x}. \tag{23}$$

This formulation is useful because the only time derivative is that of the internal energy; all other derivatives are spatial. This particular discretization of this PDE will therefore be comparatively easy to express as an ODE, since only derivatives of the internal energy with respect to the state variables are necessary.

A distinction must be drawn between the above formulation of the balance equations for an element of fluid, which has boundaries that can deform over time, and the balance equations for a fixed control volume, which has stationary boundaries. The balance equations can be converted between both frames of reference by using the Reynolds transport theorem,

$$\frac{d\Psi}{dt} = \int_V \frac{\partial(\rho\psi)}{\partial t} dV + \int_A \rho\psi(\tilde{\mathbf{v}}_\mathbf{B} \cdot \hat{\mathbf{n}}) dA. \tag{24}$$

The proper state variables with which to describe the balance equations must be chosen for each of these fixed control volumes. The state variables chosen for these models are the pressure $p$ and the *in situ* enthalpy $h$, since the equation of

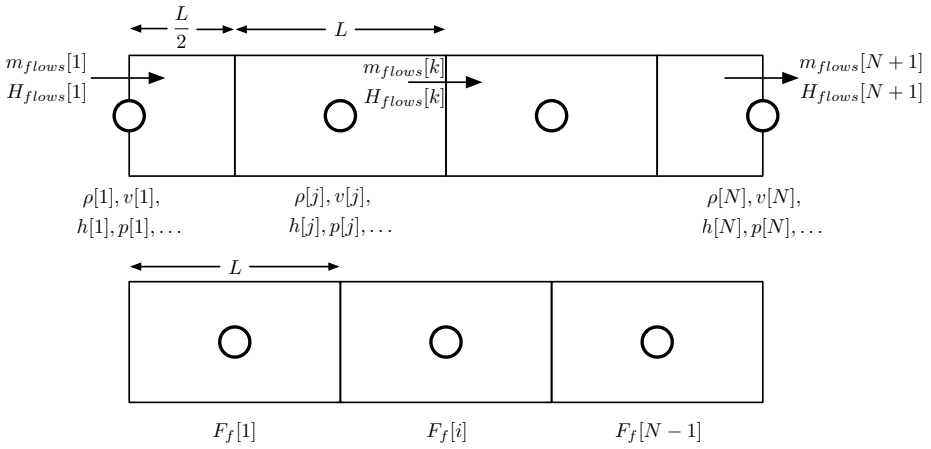


Figure 1: The staggered grids used to solve the balance equations.

state for the medium can be represented in these coordinates over the entire thermodynamic space. Expressions for the mass and total internal energy in a given fixed control volume can therefore be written as

$$\frac{d(\rho V)}{dt} = V\left(\frac{\partial \rho}{\partial p}\frac{dp}{dt} + \frac{\partial \rho}{\partial h}\frac{dh}{dt}\right) \tag{25}$$

$$\frac{d(u\rho V)}{dt} = \frac{d(\rho h - p)V}{dt} = V\left(\frac{\partial \rho}{\partial p}h - 1\right)\frac{dp}{dt} + V\left(\frac{\partial \rho}{\partial h}h + \rho\right)\frac{dh}{dt}. \tag{26}$$

The balance equations for fixed control volumes are solved on two staggered grids, as illustrated in Figure 1, to avoid the non-physical oscillatory solutions described in Patankar (1980). The mass and energy balances are solved on the upper grid, referred to as the thermal grid, while the momentum balance is solved on the lower grid, which is referred to as the momentum grid. This "staggered grid" approach is also helpful because the centers of the upper grids are aligned with the boundaries of the lower grid, so it is not necessary to interpolate properties to find the consistent values on the edges of the momentum grid. Note that there are $i = j - 1$ volumes with $j$ edges on the momentum grid.

The mass balance is only solved on the thermal grid, since all of its variables reside on this grid. Each control volume (CV) of the heat exchanger model will have mass flowing in and out; under the assumption that there are $j$ control volumes and $k = j + 1$ boundaries around those control volumes, and since the mass flow rate of refrigerant across a boundary can be written $m_{flows} = \rho A v$, the mass balance equation can be written as

$$\frac{d(\rho_j V_j)}{dt} = m_{flows,k} - m_{flows,k+1}, \tag{27}$$

where the length of integration over the control volume $L$ enters the time derivative on the left hand side, i.e., $V = LA$. The fluid properties, e.g., $\rho_j, u_j, p_j$, are evaluated in the center of each cell. By explicitly solving for the mass flow rates $m_{flows}$ on each boundary, the practice of evaluating the densities at the boundaries, rather than the middle of the cells, is avoided.

The momentum balance equation can be written in a method similar to the mass balance, resulting in

$$\frac{d(m_{flows,i}l)}{dt} = \rho_j v_j^2 A_j - \rho_{j+1} v_{j+1}^2 A_{j+1} + \frac{A_j + A_{j+1}}{2}(p_{j+1} - p_j) + F_{f,i}, \tag{28}$$

where the variables with the $j$ index are referred to the energy grid, and the variables with the $i$ index are referred to the momentum grid. The friction force $F_{f,i}$ is calculated on the momentum grid because it is related to the mass flow rates $m_{flows,i}$ and the pressure difference between the centers of the adjacent thermal grid $p_{j+1} - p_j$.

The energy balance can also be written for the thermal grid,

$$\frac{\partial(\rho_j u_j A_j)}{\partial t} = H_{flows,k} - H_{flows,k+1} + v_j A_j (p_{j+1} - p_j) + v F_{f,i} + Q_{flows,j}, \tag{29}$$

where the values of $H_{flows}$ are also computed at the edges of the control volume using the mass flow rates and the upstream convected mixed-cup enthalpy, e.g.,

$$H_{flows,k} = m_{flows,k}\bar{h}_{upstream,j}, \tag{30}$$

and the value of upstream mixed-cup enthalpy is dependent on the flow direction. For the homogeneous flow model, this is identical to the *in situ* enthalpy, but these are not equivalent in the slip flow model. As fluid passes from the two-phase region to a single-phase region, the mixed-cup enthalpy also becomes equal to the *in situ* enthalpy.

While the above discussion was focused primarily on the refrigerant side of the heat exchanger, the same approach was also used to model the air side, with the same mass, momentum, and energy balances. An ideal gas model for the air was used because there are no phase changes in the medium. This cross-flow heat exchanger was designed in a straightforward manner, and uses an ideal mixing volume to distribute the air evenly to all of the fin channels on the inlet air side of the heat exchanger and to remix the air exiting all of the fin channels on the air side outlet.

The refrigerant wall is modeled as one-dimensional heat conduction in the direction perpendicular to the refrigerant flow, with convective boundary conditions described by the refrigerant-side and air-side heat transfer coefficients, which will be given in Section 3. This wall element can be modeled simply by

$$\frac{d(m_w c_w)}{dt} = \frac{k_w A_s (T_a - T_w)}{L_w/2} + \frac{k_w A_s (T_b - T_w)}{L_w/2}, \tag{31}$$

and the surface wall temperatures $T_a$ and $T_b$ are related to the bulk temperature of the adjacent fluid by

$$Q = \alpha A (T_{fluid} - T_{surf}). \tag{32}$$

The air-side heat transfer coefficient (HTC) $\alpha$ used in these models is the enhanced Gnielinski finned tube correlation (Stephan, 2010), while the refrigerant-side HTC is set to $\alpha = 600$ W/m$^2$K for simplicity; more accurate refrigerant-side correlations will be used in future versions of these models.

The compressor model assumes there is no mass or energy storage, so the relations between the inlet and outlet variables are nonlinear and algebraic. These are given by the following standard types of relations,

$$\dot{m}_{comp} = \eta_v \rho_{suc} V f \tag{33}$$

$$h_{suc} = h_{suc} + \frac{h_{dis,isen} - h_{suc}}{\eta_{is}} \tag{34}$$

$$h_{dis,isen} = f(p_{suc}, h_{suc}), \tag{35}$$

where the functions $\eta_v$ and $\eta_{is}$ are calculated via compressor maps, and the isentropic enthalpy $h_{dis,isen}$ is calculated via the appropriate equation of state.

Lastly, a simple isenthalpic model of the expansion valve is used to describe the expansion process, with neither mass nor energy storage. The mass flow rate through the expansion device is related to the user-controlled size of the orifice in the valve, which ranged from 0 counts to 500 counts, as well as the density at the inlet of the valve and the pressure drop across the valve, e.g.,

$$\dot{m}_{EEV} = \theta \sqrt{\rho_{in}(p_{in} - p_{out})}. \tag{36}$$

# 3 IMPLEMENTATION

In principle, the system of mixture equations discussed in Section 2 describes the thermofluid dynamics for both homogeneous flow and slip flow, where the slip flow model also contains an additional closure relation that defines the slip ratio in terms of other thermodynamic variables. In practice, however, such an implementation is not computationally effective, because of the discontinuities between the single phase and two-phase regions. For example, the calculation of the slip ratio $v_G/v_L$ will go to infinity in the superheated region; this will either cause problems with numerical robustness, elicit the development of complex techniques to activate or deactivate particular equations, or some combination thereof.

One approach to address these discontinuities was proposed by Bauer (1999), in which the mean velocity $v$ and the velocity difference $\Delta v$ are used to calculate the balance equations, rather than the phasic velocities. This is done by using the expression for the mixture velocity (Equation 10) to formulate an expression for the phasic velocities, e.g.,

$$v_G = v + (1-x)(\Delta v) \tag{37}$$
$$v_L = v - x(\Delta v). \tag{38}$$

This makes it possible to express the phasic mass flow rates in terms of $v$ and $\Delta v$,

$$\dot{m}_G = \gamma \rho_G v_G A \tag{39}$$
$$= xv\rho A + x(1-x)(\Delta v)\rho A \tag{40}$$
$$= x\dot{m} + \dot{m}_{corr} \tag{41}$$
$$\dot{m}_L = (1-x)\dot{m} - \dot{m}_{corr}, \tag{42}$$

where $\dot{m}_{corr} = x(1-x)(\Delta v)\rho A$, and is calculated at the centers of each element of the thermal grid, as are all of the other thermodynamic properties. This can also be used to develop the following relation between $x$ and $\dot{x}$,

$$\dot{x} = x + x(1-x)\frac{\Delta v}{v}. \tag{43}$$

This reformulation of the phasic velocities is particularly useful because the term proportional to $\Delta v$ goes to zero both when $x \leq 0$ and when $x \geq 1$. The balance equations can be rewritten by using these expressions; the correspondingly reformulated mass balance for a fixed control volume is

$$\frac{dM}{dt} = \dot{m}_{G,in} + \dot{m}_{L,in} - \dot{m}_{G,out} - \dot{m}_{L,out} \tag{44}$$
$$\frac{d(\rho_j V_j)}{dt} = m_{flows,k} - m_{flows,k+1}, \tag{45}$$

while the modified momentum balance for the fixed control volume can be written as

$$\frac{dI}{dt} = \dot{I}_{in} - \dot{I}_{out} + (P_{in} - P_{out})A + F_f \tag{46}$$
$$\frac{d(m_{flows,i}l)}{dt} = \rho_j v_j^2 A_j + \dot{m}_{corr,j}(\Delta u)_j - \rho_{j+1} v_{j+1}^2 A_{j+1} - \dot{m}_{corr,j+1}(\Delta u)_{j+1} + \frac{A_j + A_{j+1}}{2}(p_{j+1} - p_j) + F_{f,i}, \tag{47}$$

where $I = m_{flows}l$. Finally, the energy balance for the fixed control volume can be rewritten as

$$\frac{dU}{dt} = \dot{m}_{in}\overline{h}_{in} - \dot{m}_{out}\overline{h}_{out} + \dot{Q} \tag{48}$$
$$\frac{d(\rho_j u_j A_j)}{dt} = H_{flows,k} - H_{flows,k+1} + v_j A_j (p_{j+1} - p_j) + vF_{f,i} + \dot{Q}_{flows,k} \tag{49}$$

where $H_{flow}$ is again computed using the mixed-cup enthalpy, rather than the *in situ* enthalpy. While the mass and energy balances appear to be identical to the homogeneous flow mixture equations, the phasic velocities will differ due to the non-unity slip ratio.

The Zivi (1964), Smith (1969), and Premoli *et al.* (1971) slip ratio correlations, which all use the flow quality to compute the slip ratio, were each implemented in related versions of these behavioral models. By implementing these closure relations in models which otherwise have the same underlying description of the dynamic thermofluid behavior, the effect of specific slip ratio correlations on the overall transient model behavior can be studied. Moreover, the fact that these related cycle models have different slip ratio correlations will force some model parameters, such as the total cycle charge, to take on different equilibrium values; these effects can thus be examined through the simulation of these models.

A number of important mathematical and software development techniques proved to be crucial to the successful operation of these models. These codes were developed by leveraging the relatively new `stream` operator in Modelica (Franke *et al.*, 2009a), which is used in models that involve the convective transport of properties, and makes them easier to initialize when the sign of the mass flow rate with respect to a component is not known *a priori*. This operator effectively

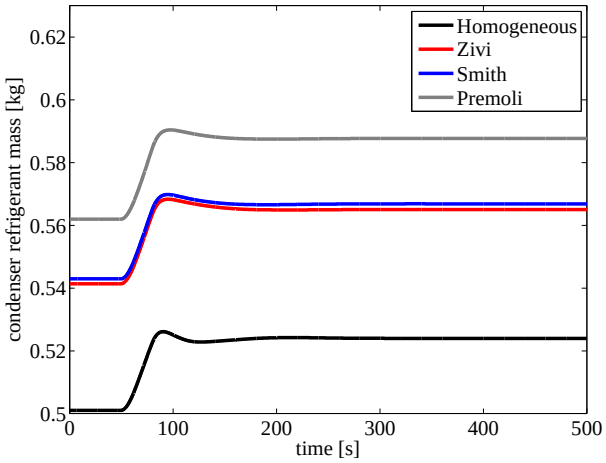


Figure 2: Condenser mass inventories for all cycle models.

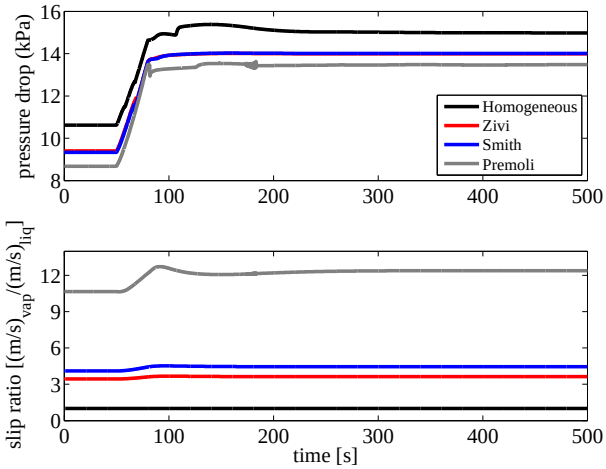


Figure 3: Pressure drop across the evaporator and slip ratio for all cycle models.

generates two sets of connection equations for every component port, one for mass flow in each direction; the compiler is then able to dynamically choose which set of equations to use when solving for the mass flow rate. In addition, the `smooth` and `noEvent` operators (Modelica Association, 2014) in Modelica were also important, because they provide a signal to the compiler when it can differentiate expressions to reduce the index of the model DAEs. Finally, unit tests were extensively utilized to troubleshoot individual models and to identify consistent sets of initial conditions when these models were combined into larger systems.

# 4 RESULTS

The models described above were implemented using the Modelica compiler Dymola 2014 and tested extensively on a set of cycle models that used R410a as a working fluid, as modeled in the commercially available Air-Conditioning Library (kn:, 2014). Each of these models was initialized from the same set of starting pressures, air-side temperatures, and mass flow rates (8 g/s), to ensure a valid basis for comparison. To illustrate the differences between these two models, one set of experiments is illustrated in Figures 2 and 3, while the related mass inventories of the cycles are listed in Table 1. At t=50 seconds during this experiment, the compressor speed was increased by a 15 second ramp from 49 Hz to 64 Hz.

| Slip ratio correlation | Cycle mass inventory |
|---|---|
| Homogeneous model | 580g |
| Zivi (1964) | 614g |
| Smith (1969) | 616g |
| Premoli *et al.* (1971) | 640g |

Table 1: Total mass inventory for simulations with different slip ratios.

It is evident from Table 1 that there are significant differences between the total mass inventory of the different cycles. Though the cycles were all initialized at the same operating point, the Premoli cycle had a total inventory that is 10.3% higher than the homogeneous flow cycle. It is also interesting to note that the Smith and Zivi cycles had similar total cycle charges, while the Premoli cycle had a 3.8% greater cycle charge than the other slip flow cycles. These differences in charge are due in part to the fact that the liquid phase velocity is much lower than the vapor phase velocity, causing the total residence time of the liquid in the heat exchangers to be much longer for the slip flow cycles than for the homogeneous flow cycle. While the basis of comparison for these simulations was the matching of the refrigerant flow rates through the heat exchangers, other strategies for model calibration, such as matching the pressure waveforms, will also have a significant effect on the total cycle charge. This reinforces the notion that the equilibrium state reached by the cycle is dependent upon the modeling assumptions made, again suggesting that the use of a slip flow model is important when it is applicable.

Figures 2 and 3 demonstrate the effect of the different slip ratios on the transient response of the system. In particular, it is interesting to note in Figure 2 that the transient response of the condenser mass inventory for the homogeneous cycle is more underdamped than the equivalent responses for the slip flow models. In Figure 3, it can be seen that the pressure differences across the evaporator and the shapes of the pressure transient caused by the change in the actuators are similar, suggesting that not all of the dynamics of the system are dependent upon the slip flow model. This result is encouraging, as it echoes previous work in the modeling of evaporators. While there are some differences in the shapes of these transients, more work must be done to determine if these features are physical or numerical in nature. Finally, it is interesting to note that the choice of the slip flow model has a significant effect on the size of the slip ratio transients; the slip ratio for the Premoli cycle has a much larger transient than the other two cycles. Future studies of this dynamic effect in experimental data may provide further information about the actual sizes of these slip ratio transients, which could in turn be used for other modeling studies and correlation development.

# 5 CONCLUSIONS AND FUTURE WORK

In this paper, a heterogeneous slip flow model for two-phase heat exchangers was proposed, and a Modelica implementation of two complete cycle models with different flow assumptions were discussed. In comparing the characteristics of these cycle models it is clear that the slip flow cycle models have a higher refrigerant mass inventory than the homogeneous model, even though the evaporator pressure dynamics of both models are similar. On the basis of these results, it is clear that the some of the differences between the cycles with either homogeneous flow or slip flow are not negligible, and that the flow model must be carefully considered when developing models, especially those which will be calibrated to experimental data. Further work in this area could include the validation of the complete cycle data against an experimental heat pump system, as well as the further refinement of these models, such as incorporation of more accurate correlations.

# ACKNOWLEDGEMENTS

The author would like to thank Huize Li for his excellent work and assistance in the early stages of developing these models.

# NOMENCLATURE

| | | | | | |
|---|---|---|---|---|---|
| $A$ | cross-sectional area | $k$ | thermal conductivity | $\psi$ | intensive property |
| $D$ | tube diameter | $\dot{m}$ | mass flow rate | **Subscript** | |
| $F$ | force | $p$ | pressure | $k, i, j$ | control volume index |
| $I$ | momentum | $u$ | specific internal energy | $dis, isen$ | isentropic discharge |
| $L$ | wall thickness | $v$ | velocity | $suc$ | suction port |
| $M$ | mass | $x$ | static quality | $dis$ | discharge port |
| $Q$ | heat flow rate | $\dot{x}$ | flow quality | $G$ | gas |
| $S$ | slip ratio ($=v_G/v_L$) | $\alpha$ | heat transfer coefficient | $L$ | liquid |
| $T$ | temperature | $\gamma$ | void fraction | $b$ | bulk |
| $U$ | internal energy | $\zeta$ | friction factor | $corr$ | correction |
| $V$ | volume | $\eta$ | efficiency | $a$ | air |
| $c$ | specific heat capacity | $\rho$ | density | $w$ | wall |
| $\underline{h}$ | *in situ* specific enthalpy | $\theta$ | EXV stroke fraction | $f$ | friction factor |
| $h$ | "mixed-cup" specific enthalpy | $\Psi$ | extensive property | | |

# REFERENCES

*Air Conditioning Library User Guide*. Modelon (2014). v1.8.4.

Bauer, O. *Modeling of Two-Phase Flows in Modelica*. Master's thesis, Lund Institute of Technology (1999).

Bonilla, J., Yebra, L., and Dormido, S. Chattering in dynamic mathematical two-phase flow models. *Applied Mathe-*

*matical Modeling*, 36:2067–2081 (2012).

Cellier, F. and Kofman, E. *Continuous System Simulation*. Springer (2006).

Elmqvist, H., Tummescheit, H., and Otter, M. Object-oriented modeling of thermo-fluid systems. In *Proceedings of the 3rd Modelica Conference* (2003).

Franke, R., Casella, F., Otter, M., Sielemann, M., Elmqvist, H., Mattson, S.E., and Olsson, H. Stream connectors: An extension of Modelica for device-oriented modeling of convective transport phenomena. In *Proceedings of the 7th Modelica Conference* (2009a).

Franke, R., Casella, F., Sielemann, M., Proelss, K., Otter, M., and Wetter, M. Standardization of thermo-fluid modeling in Modelica.Fluid. In *Proceedings of the 7th Modelica Conference* (2009b).

Ghiaasiaan, S. *Two-Phase Flow, Boiling, and Condensation in Conventional and Miniature Systems*. Cambridge University Press (2007).

Harms, T., Groll, E., and Braun, J. Accurate charge inventory modeling for unitary air conditioners. *HVAC&R Research*, 9(1):55–78 (2003).

Ishii, M. and Hibiki, T. *Thermo-Fluid Dynamics of Two-Phase Flow*. Springer, 2 edition (2011).

Kærn, M. *Analysis of flow maldistribution in fin-and-tube evaporators for residential air-conditioning systems*. Ph.D. thesis, Technical University of Denmark (2011).

Kapadia, R., Jain, S., and Agarwal, R. Transient characteristics of split air-conditioning systems using R22 and R410a as refrigerants. *HVAC&R Research*, 15(3):617–649 (2009).

Kolev, N. *Multiphase Flow Dynamics 2*. Springer (2005).

Li, B. and Alleyne, A. A dynamic model of a vapor compression cycle with shut-down and start-up operations. *International Journal of Refrigeration*, 33(3):538–552 (2010).

Li, P., Li, Y., Seem, J., Qiao, H., Li, X., and Winkler, J. Recent advances in dynamic modeling of HVAC equipment. Part 2: Modelica-based modeling. *HVAC&R Research*, 20(1):150–161 (2014a).

Li, P., Qiao, H., Li, Y., Seem, J., Winkler, J., and Li, X. Recent advances in dynamic modeling of HVAC equipment. Part 1: Equipment modeling. *HVAC&R Research*, 20(1):136–149 (2014b).

Ma, X., Ding, G., Zhang, P., Han, W., Kasahara, S., and Yamaguchi, T. Experimental validation of void fraction models for R410a air conditioners. *International Journal of Refrigeration*, 32:780–790 (2009).

Modelica Association. Modelica specification, version 3.3 (2014).

Mortada, S., Zoughaib, A., Clodic, D., and Arzano-Daurelle, C. Dynamic modeling of an integrated air-to-air heat pump using Modelica. *International Journal of Refrigeration*, 35(5):1335–1348 (2012).

Patankar, S. *Numerical Heat Transfer and Fluid Flow*. Hemisphere Publishing Co. (1980).

Premoli, A., Francesco, D., and Prina, A. A dimensional correlation for evaluating two-phase mixture density. *La Termotecnica*, 25:17–26 (1971).

Rasmussen, B. Dynamic modeling for vapor compression systems. Part 1: Literature review. *HVAC&R Research*, 18(5):934–955 (2012).

Smith, S. Void fractions in two-phase flow: A correlation based upon an equal velocity head model. *Proc. Inst. Mech. Eng.*, 184:647–664 (1969).

Stephan, P., editor. *VDI Heat Atlas*. Springer-Verlag (2010).

White, F. *Fluid Mechanics*. McGraw-Hill, 6th edition (2008).

Willems, J. The behavioral approach to open and interconnected systems. *IEEE Control Systems Magazine*, 27:46–99 (2007).

Zivi, S. Estimation of steady-state steam void fraction by means of the principle of minimum entropy production. *J. Heat Transfer*, 86:247–252 (1964).